Journal of Electroanalytical Chemistry 964 (2024) 118341

Contents lists available at ScienceDirect

Journal of Electroanalytical Chemistry

journal homepage: www.elsevier.com/locate/jelechem

Spectroscopic investigations of a commercial graphite screen printed electrode modified by bismuth oxide drop deposition and electrochemical reduction, for cadmium and lead ions simultaneous determination

Angelantonio De Benedetto [a], Antonio Della Torre [b], Maria Rachele Guascito [c], Riccardo Di Corato [b,d], Laura Chirivì [a], Rosaria Rinaldi [a,b], Alessandra Aloisi [b,*]

[a] Mathematics and Physics "E. De Giorgi" Department, University of Salento, Via Monteroni, Lecce 73100, Italy
[b] Institute for Microelectronics and Microsystems (IMM), CNR, Via Monteroni, Lecce 73100, Italy
[c] Biological and Environmental Sciences and Technologies Department, University of Salento, Via Monteroni, Lecce 73100, Italy
[d] Center for Biomolecular Nanotechnologies, Istituto Italiano di Tecnologia, Arnesano 73010, Italy

ARTICLE INFO

Keywords:
Graphite
Bismuth oxide
micro-X-ray fluorescence
X-ray photoelectron spectroscopy
Ground water
Heavy metal

ABSTRACT

A single use graphite screen-printed electrode (GSPE) was easily modified, to take advantage of the proven affinity of the nontoxic post-transition metal bismuth (Bi), for metal ions to be detected by Square Wave Anodic Stripping Voltammetry (SWASV). A bismuth oxide (Bi_2O_3) or a chitosan coated (CS@Bi_2O_3) nanopowder suspension was drop-casted on the graphite working electrode (WE) surface, giving rise to the precursor of a Bi-modified GSPE. After that, an electrochemical reduction was performed to obtain the Bi– or the CS@Bi–GSPE.

X-ray photoelectron spectroscopy and micro-X-ray fluorescence investigations were performed on the graphitic structure pre and post modification. The bismuth oxide deposition amount was considered as critical parameter to sensor performance, indicating a minimum and maximum threshold. Under improved measurement conditions, with a 300 s pre-concentration time, the attained sensors exhibited a linearity in the range (2.0–20.0) μg L^{-1} in the simultaneous analysis of Pb(II) and Cd(II). The Bi–GSPE showed LODs of 1.7 and 0.5 μg L^{-1} for Cd (II) and Pb(II) respectively, while 1.5 μg L^{-1} for Cd(II) and 0.2 μg L^{-1} for Pb(II) were recorded by the CS@Bi–GSPE. As an applicative proof in real sample, a spike test was carried out in a ground water sample, without any preliminary sample treatment.

1. Introduction

Protecting groundwater, for environment, animal, and human health, requires analyzing hazards to groundwater quality. There is a close link between assessing pollution potential and monitoring, as preliminary surveys of groundwater quality and contamination sources are both important to support parameter selection for long-term routine groundwater quality observing programmes [1]. In-situ monitoring of metal contaminants in water, by voltammetric methods, represents reliable and economic analytic procedure for active and cost- effective monitoring. Mercury based electrodes have been the transducer of choice in stripping voltammetry of trace metals for a long time due to their sensitivity, reproducibility, and renewability. In the context of green analytical chemistry, bismuth-based electrodes provide a valuable and widely used alternative. Relying on a bismuth or bismuth-modified active surface, these electrodes are comparable in terms of analytical performance, while they are characterized by minor toxicity in comparison to their mercury counterparts [2]. The stripping performance of bismuth electrodes reflects the ability of bismuth to form multicomponent alloys/intermetallic compounds with heavy metals [3] and voltammetric determination of heavy metals by stripping analysis strongly depends on the properties of the WE, where a "pre- concentration" step of the analyte is applied [4,5]. Commonly utilized carbon based electrodes (glassy carbon electrode, graphite electrode, carbon paste electrode, and screen-printed carbon electrode) for voltammetric determination of heavy metals, hold desirable conductive and surface properties that allow sensitive determination of analytes [6] To advance the preparation of non-mercury sensors, more than a few modification procedure have been developed since the first use of a bismuth-coated electrode in electrochemical stripping analysis which was presented at

* Corresponding author.
E-mail address: alessandra.aloisi@cnr.it (A. Aloisi).

https://doi.org/10.1016/j.jelechem.2024.118341
Received 8 February 2024; Received in revised form 3 May 2024; Accepted 12 May 2024
Available online 13 May 2024

the forum of Young Investigators on Analytical Chemistry in 2000 [7].

In the plating process, Bi(III) ions are added to the sample solution and metallic bismuth is electrochemically deposited on the electrode surface during the analysis (in-situ plating) [8], or it is electrochemically deposited before placing the electrode in the sample solution for measurements (ex-situ plating) [9]. Alternatively, by sputtering bismuth onto a silicon or ceramic substrate a bismuth thin film is obtained [10,11]. Other strategies involve surface drop casting of bismuth-based modifier suspensions [11] as well mixing bismuth precursors (i.e. bismuth oxide, bismuth citrate, bismuth aluminate) and graphite ink in the bulk method for SPE fabrication process [8,12,13].

Likewise, nanomaterials are ideal elements for modifying the surface of the electrodes via dropping and deposition, moreover they are appropriate for use in electrochemical systems to determinate metal ion concentration owing to their unique properties, such as large specific surface area, large number of adsorption-active sites, high electronic conductivity, good chemical stability, selectivity and reproducibility [14].

One of the first remark on the term "nano" in electroanalysis with bismuth electrodes belongs to disposable thick-film sensors with Bi-nanolayer assembled from a modifier ($BiPO_4$); since 2000, many Bi-nanomaterial modified electrodes have been and are being produced with successful results [15,16].

In a context of still growing interest for Bi-based electrodes, in the present work, a simple, rapid, and cost-effective modification of a commercial GSPE was studied and tested for the simultaneous detection of Cd(II) and Pb(II) ions in water samples. It was basically achieved by drop casting a bismuth oxide nanopowder (diameter range, 80–200 nm) suspension or chitosan covered bismuth oxide nanostructures onto the WE activated surface. In compliance with the parameters to be considered when developing heavy metal electrochemical sensors [17], the achieved LODs of 1.5 and 0.2 μg L^{-1}, for Cd(II) and Pb(II) correspondingly, were well below the guideline values for groundwater bodies and drinking water pollution monitoring indicated by last EU Directive [18] and WHO Water Safety Plan [19] as "5 μg L^{-1} and 10 μg L^{-1} (5 μg L^{-1} by January 2036)", respectively for cadmium and lead. Besides, a deep spectroscopical characterization of the commercial GSPE composition was conducted to better investigate and support the improvements attained with our bismuth modification approach.

2. Material and methods

2.1. Chemicals and solutions

All the chemicals employed were used as received: bismuth (III) oxide nanopowder (80–200 nm) (Alfa Aesar, 46314), potassium hydroxide, acetic acid, chitosan low molecular weight (CS-LMW) (Aldrich) sodium acetate anhydrous (Fluka), potassium chloride (P5405 Sigma), VWR Standard solution of lead (Pb) and cadmium (Cd) for AAS (1 g/L in 2 % HNO_3 matrix). Standard solutions were prepared daily and diluted as needed from 5 mg/L stock solution prepared in the specific buffer. Ultrapure water with a resistivity of 18.2 MΩ cm collected from a water purification system (Thermo Scientific Barnstead Smart2Pure) was employed in all experiments. All the experiments were conducted at room temperature (approximately 25 °C) without removing the dissolved gases.

2.2. Sensors and apparatus

Disposable screen-printed sensors (3-electrode system with graphite working and counter electrode (WE, CE), and silver pseudo-reference electrode (RE)) were from (ItalSens IS-C SPE). Electrochemical measurements were carried out by PalmSens4 potentiostat/galvanostat/impedance analyzer (PalmSens BV) controlled by PSTrace 5 software, in glass vials positioned on a magnetic stirrer (IKA RCT basic). Reference Electrode (ItalSens) Ag/AgCl in aqueous KCl was used in the chronoamperometry during the WE modification steps and in the cyclic voltammetry measurements.

2.3. Procedure: Optimized working conditions

Two supporting electrolyte solutions were prepared to optimize the electrochemical analysis: a KCl 0.1 M solution acidified with HCl to reach a pH of 2.2 and a buffer acetate solution pH 4.5 (with a final sodium acetate concentration of 0.1 M) having a KCl concentration of 0.03 M. By a serial dilution of the standard solutions in the specific buffer, 5 mL of each solution were poured into a glass vial, placed over the stirrer and the SPE was vertically immersed. After connecting the electrode to the potentiostat, SWASV measurements were carried out as it follows. A deposition potential of −1.2 V was applied for 5 min under stirring condition. Then, the equilibration step was performed by stopping the stirrer and applying the same potential for 20 s. The SWV was performed with a potential sweep from −1.2 V to −0.3 V (equilibration time of 2 s, step potential of 2 mV, amplitude of 50 mV and frequency of 35 Hz). Before the deposition step, two conditioning steps were executed under stirring condition by applying a potential of −0.4 V for 2 min (first step) and 1 min (second set) with each step followed by SWV potential sweep from −1.2 V to −0.3 V. To analyze the current behavior during the deposition, equilibrium and conditioning phases, the applications of the −1.2 V and −0.4 V potentials were performed by chronoamperometry (interval time of 0.5 s and equilibration time of 2 s). All applied potentials were referred to the Ag pseudo-reference electrode.

2.4. Activation step

Taken as received, the graphite WE shows a hydrophobic surface, so it was necessary to perform an activation step in order to allow successive drop casting of the aqueous colloidal suspension. It was observed that, applying a potential of + 1.6 V (vs. Ag/AgCl RE) for 2 min in KOH 0.01 M solution, it was enough to achieve the desired wettability. It is reasonable that oxidative changes occurring in the graphite surface contribute to this end [20].

2.5. Modification of the WE with bismuth oxide

A homogeneous suspension with a concentration of 0.33 mg/mL of bismuth oxide was prepared by mixing bismuth oxide and KOH 0.01 M solution followed by sonication at 40 kHz for 30 min. KOH solution was used because the bismuth oxide is stable in most neutral and alkaline aqueous solutions free from reducing agents [21]. Then, 5 μL of the suspension were deposited on the WE using a micropipette and allowed to dry at 60 °C, for 10 min. Finally, to obtain the bismuth layer on the WE surface by reduction of the oxide, the SPE was immersed in KOH 0.1 M and a potential of −1.2 V (vs Ag/AgCl RE) was applied for 5 min.

2.6. Modification of the WE with chitosan coated − bismuth oxide nanostructures

A suspension of bismuth oxide nanostructures coated with chitosan (CS@Bi_2O_3 NS) was prepared in ultrapure water. Bismuth oxide NSs (0.5 mg/mL) in ultrapure water were sonicated at 40 kHz for 30 min. Chitosan powder (2 % w/v) in 0.6 M acetic acid was stirred until a clear solution was obtained. Then, 120 μL of chitosan solution were added to 1.5 mL of bismuth oxide suspension and the obtained mixture was stirred for 24 h. After that, the CS@Bi_2O_3 NSs were centrifuged and resuspended in ultrapure water for three cycles. The resulting NS suspension was measured in terms of Z potential, resulting in a positive value ((28 ± 2) mV) vs the negative one of Bi_2O_3 NPs which were measured both in acidic ((–23 ± 1) mV) and alkaline ((−49.6 ± 0.3) mV) condition. To modify the WE, 5 μL of the obtained suspension were drop casted on the activated electrode surface and allowed to dry at 60 °C for 10 min. The reduction of Bi_2O_3 in KOH 0.1 M was carried out

by applying a potential of −1.2 V (vs Ag/AgCl RE) for 5 min.

2.7. Micro X-ray fluorescence measurements

μXRF is a technique that can perform spot analysis, line scan and mapping of elements at high spatial resolution. A spectroscopic analysis of a) activated graphite WE, b) activated WE modified with Bi_2O_3 or c) activated WE modified with CS@Bi_2O_3 after reduction, was performed by a μ-XRF (Orbis PC Edax / Ametek) under a vacuum condition.

Primary X-rays are generated in the X-ray tube with rhodium as the target anode and the characteristic X-rays emitted by the sample are detected by a silicon/lithium detector. To obtain optimal spectral information various operating parameters were varied. Finally, the measurements were carried out with the time constant of 12.8 μs, dwell time of 400 ms and matrix size of 128 × 100 pixels, using 40 kV of beam voltage, 550 μA of beam current, spot size of 30 μm and a Nichel filter of 25 μm. The applied filter removes primary photons with energies interfering with fluorescence photons from the element of interest, thus resulting in lower background scattering in the spectrum. The quality of the measured data was valued from its signal-to-noise ratio (SNR). Besides, when evaluating an XRF spectrum, the SNR offers objective determination in peak searching. An element is present, and its peak may be identified in the XRF spectrum if the SNR is three or greater. So that the element is considered to be present at a concentration that is higher than the background noise by a statistically significant amount [22]. Then, to better investigate the elemental composition of the commercial GSPE, a line scan of WE, CE and RE was conducted in plan (figure SI1).

2.8. XPS measurements

Elemental atomic composition and chemical surface speciation of graphite WE, as provided and after oxidation in KOH 0.01 M, WE/Bi_2O_3 and WE/CS@Bi_2O_3 were determined by an AXIS ULTRA DLD (Kratos Analytical) spectrometer for X-ray photoelectron spectroscopy (XPS) analysis. An Al Kα (1486.6 eV) monochromatic source, operating at 10 kV and 15 mA, was employed during the analysis. The pressure in the analysis chamber was in average 1.3 x 10^{-9} Torr. Spectra acquisition was made in a fixed analyzer transmission (FAT) mode, at pass energy of 160 eV for survey scan (step size 1 eV) and 20 eV for high-resolution (HR) spectra acquisition (step size 0.1 eV). The sampled area was 700 μm × 300 μm. The experimental binding energy values were corrected by setting the binding energy of C1s hydrocarbon photo-electron line at 285.0 eV used as an internal standard [23,24]. Data analysis was performed using the fitting program CASA-XPS. Peaks were assigned based on literature data and on the NIST standard reference database [25]. Peak areas were converted to atomic percent (At%) using established procedures and the appropriate sensitivity factors (SF) to ensure the correct elemental mass balance, in the limit of our accuracy [26]. All obtained atomic percentage compositions were representative of the mean values obtained on minimum three different spots of the same sample.

3. Results and discussion

3.1. Relation between amount of bismuth oxide deposition and sensor performance

The amount of WE-modifying material considerably affects the stripping response. To estimate the effective amount of bismuth oxide to be deposited on the WE, several electrodes modified with different concentration of the suspension were tested for the detection of 20 μg L^{-1} of Cd(II) and Pb(II) in KCl 0.1 M pH 2.2. As shown in the Figs. 1 and 2, it was observed that the amount of deposited Bi_2O_3 on the WE surface affects the response of the electrode in heavy metal detection, concerning current peak amplitude and relative errors (based on 3 measurements). At lower amount of Bi_2O_3, the graphite surface is more exposed; in this condition, the current intensity for Pb(II) is higher than that recorded for Cd(II), probably due to a more favorable lead ion-graphite than cadmium ion-graphite interaction, as it happens with non modified graphite sensor (Figs. 10, 11). The highest current peak amplitudes were obtained for bismuth oxide concentrations of 0.33 and 0.5 mg/mL. No relevant change in relative errors was observed for Cd (II), whereas for Pb(II) a decrease in the value of relative errors was observed as the concentration of bismuth decreased. Based on that, to modify the WE it was decided to use a suspension with a bismuth oxide working concentration of 0.33 mg/mL (nanopowder suspension morphology is showed in Fig. 2).

It was observed that the bismuth layer is more necessary for the detection of Cd(II), and that the amount and distribution of its deposition on the activated graphite surface can affect the reproducibility of the measurements. The amplitude of the Pb peak may be due to two contributions: that due to the interaction of Pb(II) with the deposited bismuth and that due to the deposition of Pb(II) on the graphite surface. In fact, as observed in Figs. 10 and 11, bare graphite is enough to detect Pb as low as 5 μg/L with respect to Cd. It may be that at low Bi2O3 concentrations, the amplitude of the Pb(II) peak is mainly due to graphite alone, so the relative error due to Bi2O3 deposition is reduced because the contribution given by graphite is greater than that given by bismuth. The relative error of Cd is around 20 %, and a trend like that of Pb(II) is not recorded because the relative peak of Cd(II) depends on with bismuth interaction.

3.2. Cyclic voltammetry of bismuth oxide modified SPE

Fig. 3 show the voltammograms obtained in KOH 0.1 M of the

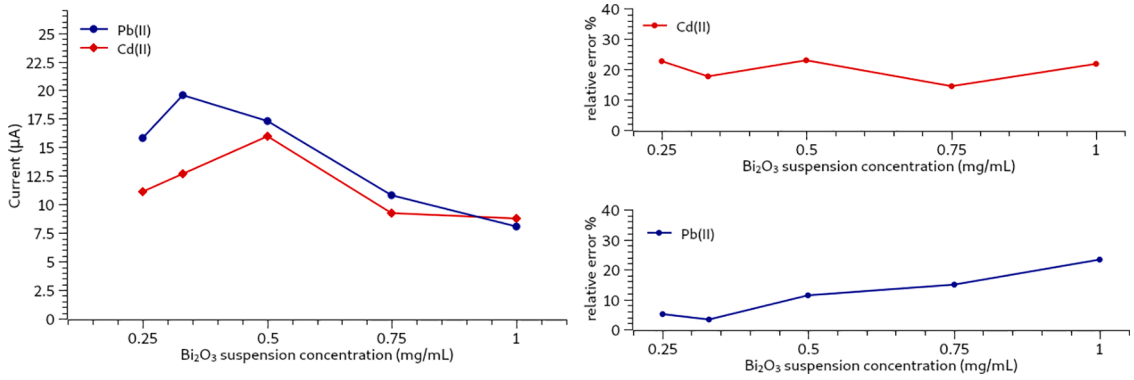

Fig. 1. Anodic stripping SWV. SPE response as a function of concentration of bismuth oxide deposited on the WE in the detection of 20 μg L^{-1} of Cd(II) and Pb(II) in KCl 0.1 M pH 2.2. Current peak amplitudes (left) and relative errors (right).

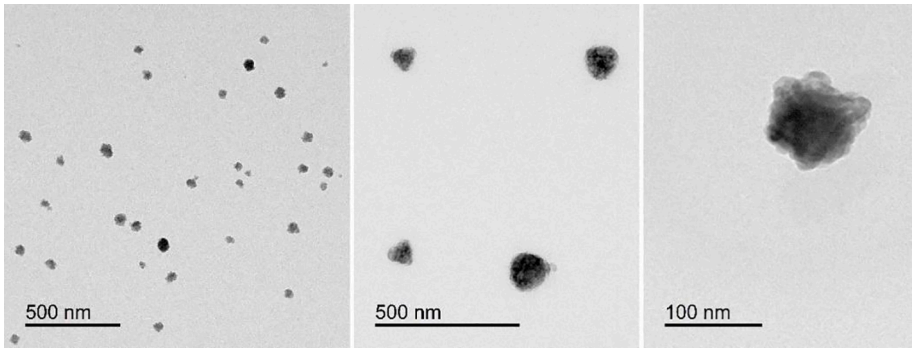

Fig. 2. TEM image of the commercial bismuth oxide nanopowder, sample (few microliters dropped onto a carbon-coated copper grid.) from the working suspension (0.33 mg/mL Bi_2O_3 – KOH 0.01 M), showing particles diameters under 100 nm with no microaggregates. The analysis has been performed by a JEOL JEM-1011 TEM, operating at an accelerating voltage of 100 kV.

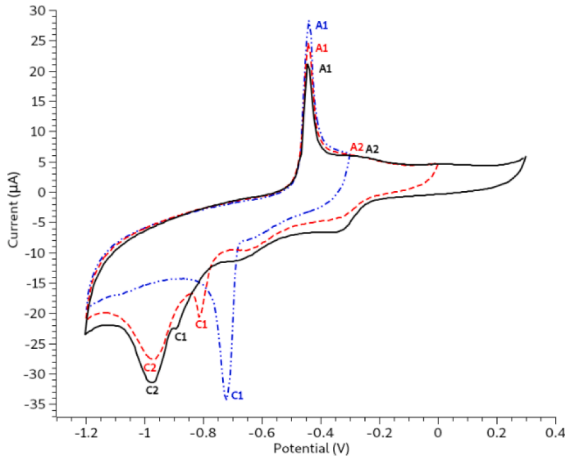

Fig. 3. Voltammograms of the activated GSPE modified with Bi_2O_3 in KOH 0.1 M. A first cyclic scan from −0.3 V to −1.2 V (vs Ag/AgCl RE) (blue dash dot dot line), a second cyclic from 0 V to −1.2 V (vs Ag/AgCl RE) (red dashed line) and a third cyclic scan (black line) from 0.3 V to −1.2 V (vs Ag/AgCl RE) are shown.

bismuth oxide modified graphite electrode. A first cyclic scan from −0.3 V to −1.2 V (vs Ag/AgCl RE) (blue dash dot – dot line) showed a cathodic peak (C1) and an anodic peak (A1). A second cyclic scan from 0 V to −1.2 V (vs Ag/AgCl RE) (red dashed line) showed another cathodic peak (*C2*) and a decrease in the amplitude of the C1 peak and its shift towards more negative potentials. In addition, a decrease in the amplitude of the A1 peak was also observed. A third cyclic scan from 0.3 V to −1.2 V (vs Ag/AgCl RE) (black line) showed an additional shift to more negative potentials for peak C1, whereas no shift was observed for peak *C2*. An additional decrease in the amplitude of peaks C1 and A1 was also observed.

In alkaline media, Bi_2O_3 can slightly dissolve giving Bi_2O^-. In the cathodic scan, the C1 peak should be related to the reduction of the adsorbed BiO_2^- (eq. 2, 3 and 4) and *C2* peak should be related to the main process and to the largest amount of exchanged charges. (it could correspond to eq. 1, 2, 3 and 4). The reactions 2 and 3 are equivalent to a multiple electron exchange [27,28].

$$Bi_2O_3 + 2OH^- \rightarrow 2BiO_2^- + H_2O \quad (1)$$

$$BiO_2^- + e^- \rightarrow BiO_2^{2-} \quad (2)$$

$$2H_2O + 3BiO_2^{2-} \leftrightarrows 2BiO_2^- + 4OH^- + Bi^0 \text{ (disproportionation)} \quad (3)$$

Bi^0 (the Bi element at 0 oxidation degree), polycondenses with other ones giving the metal Bi [27]:

$$Bi^0 \rightarrow Bi_{met} \text{ (formation of bismuth metal lattice)} \quad (4)$$

In the anodic scan, the A1, A2 peaks and the region following the A2 peak between the potential values of −0.15 V and 0.3 V, showed in the Fig. 3, should be related to oxidation reactions that could correspond to the following ones [27,28]:

$$Bi_{met} \rightarrow Bi^+ + e^- \quad (5)$$

$$3Bi^+ \leftrightarrows Bi^{3+} + 2Bi_{met} \quad (6)$$

$$3OH^- + Bi^{3+} \rightarrow Bi(OH)_3 \quad (7)$$

$$Bi(OH)_3 + OH^- \rightarrow BiO_2^- + 2H_2O \text{ (dissolution)} \quad (8)$$

With respect to the activated bare graphite electrode (Fig. 4), a clear cathodic peak (C0) was observed in the three cyclic scans in KOH 0.1 M. As well, increase in the amplitude of the C0 peak was observed with increasing the range of the anodic scan.

The C0 peak may be due to the reduction of oxygen [29] (dissolved oxygen in the solution) at the graphite surface of the WE under condition of higher pH. The C0 cathodic peak, around the potential value of −0.3 V, was also present in the voltammogram in Fig. 3 because, as can be observed from the XRF analysis (Fig. 5b) the WE was not completely covered by bismuth nanostructures after the modification step performed on the activated graphite.

3.3. Elemental composition of modified SPE WE by micro-X-ray analysis

XRF spectra and relative maps derived from a square area of

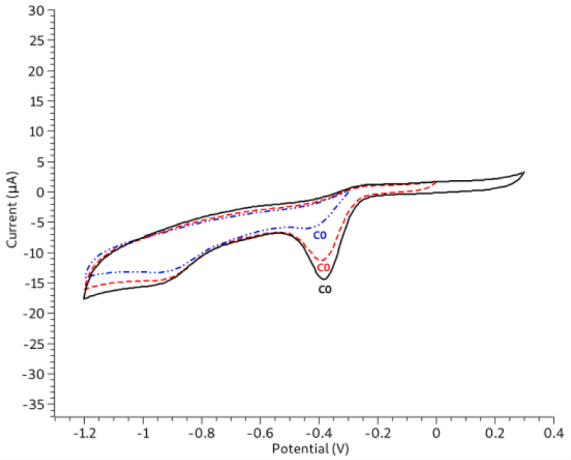

Fig. 4. Voltammograms of the bare activated GSPE. First cyclic scan from −0.3 V to −1.2 V (vs Ag/AgCl RE) (blue dash dot dot line), second cyclic from 0 V to −1.2 V (vs Ag/AgCl RE) (red dashed line) and third cyclic scan (black line) from 0.3 V to −1.2 V (vs Ag/AgCl RE).

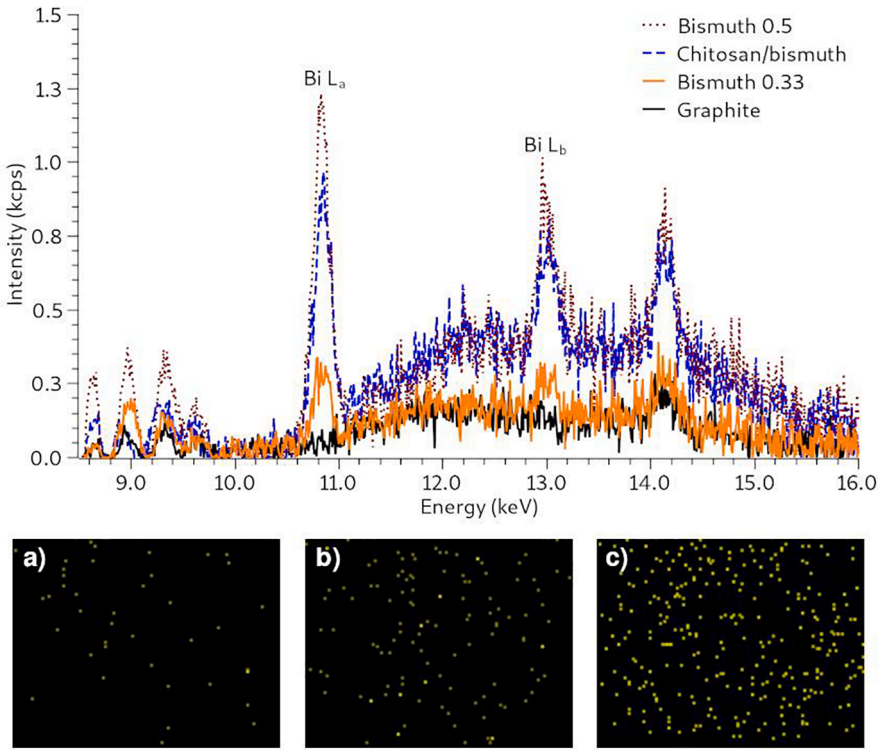

Fig. 5. Spectrum mapping of the graphite SPE working electrode and μ-X-ray map of bismuth distribution in the working electrode area (~7 mm^2) of activated graphite WE (a), modified with Bi_2O_3 (b) or CS@Bi_2O_3 NSs (c) after reduction.

approximately 7 mm^2 inscribing the circular area of activated graphite WE, and WE modified with Bi_2O_3 or CS@Bi_2O_3 NSs after the reduction step (Fig. 5) show the availability of the Bi metallic element.

As reported previously, a spectral peak may be labeled when its SNR is three or greater offering further objectivity in peak identification/label decisions [22]. We calculated a SNR value for WE graphite lower than 3 as we expected, while for WE/Bi_2O_3 (orange line) and WE/CS@Bi_2O_3 (blue dash line) the values were greater than three (13.2 and 18, respectively) confirming the consistency about peak identification/labels for bismuth element. The spectrum mapping of activated graphite WE (a), modified with Bi_2O_3 (concentration of 0.33 mg/mL) (b) or CS@Bi_2O_3 NSs (concentration of 0.5 mg/mL) (c) after reduction show the pixel distribution for bismuth that is almost insignificant as expected in (a), and uniformly distributed in (b) and (c).

3.4. Elemental composition of modified SPE WE by XPS analysis

X-ray photoelectron spectroscopy (XPS) analysis was used to characterize the graphitic SPE modified WE electrodes in different electrochemical treatments to monitor their surface chemical composition. The survey spectra of the modified WE with Bi_2O_3, with and without chitosan, are reported in figure SI2. As expected, the HR of carbon (C1s) and oxygen (O1s) photoelectron peaks (Fig. 6), show that the surface of the SPE WE as furnished and after anodic oxidation pretreatment are chemically different in terms of carbonaceous and oxygenated components contribution. The XPS results (Table SI 1) show the as furnished GSPE WE surface to be composed of 87.47 % carbon and 6.58 % oxygen ((At%)C /(At%)O ratio of 13.3) with the C1s spectrum typical of an oxidized graphite-like material [30]. The Cl2s in C1s region, coupled with Cl2p (not shown) chloride signal at 199.7 ± 0.1 eV (At% of 5.5) from PVC are also present. The C1s related fitted spectrum (figure SI3, panel A) shows a strong and narrow component at approximately 284.2 ± 0.1 eV binding energy (49.5 At%), which is typical of graphitic carbon (Csp^2). The component at 285.00 ± 0.1 eV (17.84 At%) is attributed to Csp^3 bond (C—C(H)). The characteristic ratio (At%)$_{Csp2}$/(At%)$_{Csp3}$ is in average 2.8 according to Morgan 2021 [31]. At higher binding energy, the peak at 286.1 ± 0.1 eV is due to carbon in either PVC (C-Cl) or epoxy/alkoxy groups (C—O/C—O—C), which cannot

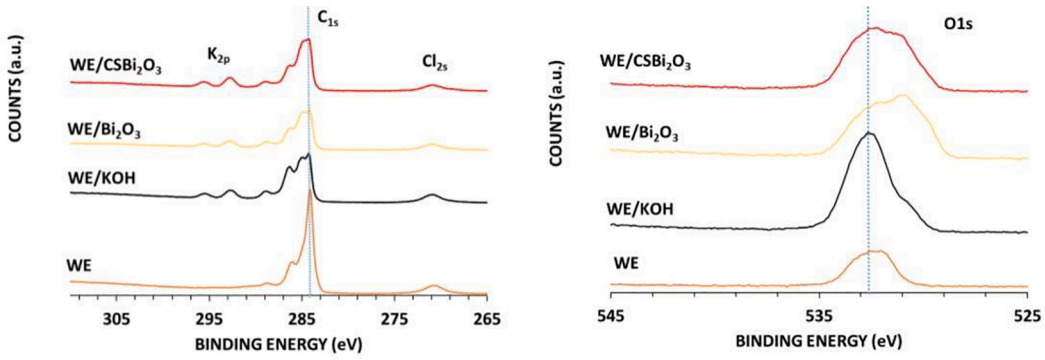

Fig. 6. HR XPS spectra of WE, WE/KOH, WE/Bi_2O_3 and WE/CS@Bi_2O_3 samples showing C1s, K2p, Cl2s and O1s regions.

generally be resolved by XPS [30]. Components at 288.9 ± 0.1 eV and 290.5 ± 0.1 eV, have been attributed to shake-up in π-π bonds of graphitic structure. However, a contribution of carboxylic carbon (–C**O**OH) at 288.9 ± 0.1 eV cannot be excluded. The presence of oxygenate carbonaceous species is confirmed by the corresponding presence of O1s peaks [30] at 531.8 (–C=**O**) and 532.9 eV (C—**O**/C—**O**—C) (figure SI3, panel A'). The chemically pretreated electrode surface, at + 1.6 V vs Ag/AgCl RE in KOH 0.01 M, had a reduced carbon content of 73.76 % and an increased oxygen content of 18.21 %, indicative of the oxidation induced on the electrode surface where the $(At\%)_C/(At\%)_O$ is reduced to 4. Chloride signal at 199.9 ± 0.1 eV (At % of 5.5) is still present, now accompanied by K2p and F1s peak signals, where potassium species can be attributed to residual contamination from KOH electrolyte, while the fluorine traces (<0.7 %) can be associated to the support material of GSPE. Related data are reported in Table SI1. The fitted C1s spectrum from the GSPE pretreated electrode is reported in figure SI3, panel B. The spectrum shows a reduced narrow component at approximately 284.2 ± 0.1 eV binding energy of the graphitic carbon (13.1 At%) to respect pristine one with a strong increment of the component Csp^3 at 285.0 eV (31.0 At%) that suggests a heavy contamination process induced by the pretreatment in KOH. The contribution from chloride in PVC is always of 5.51 At%. The increment in terms of oxygen content is associated to the increment of the carbonaceous oxidized components at respectively 286.4 ± 0.1 eV (**C**—O/**C**—O—**C**), 287.7 ± 0.1 eV (—**C**=O) and 288.9 ± 0.1 eV (—**C**OO^-). Based on the O1s most intense peak at 532.7 ± 0.1 eV (figure SI3, panel B') the prevailing oxidized forms is the singly bound oxygen (i.e. epoxy, alkoxy groups) [23]. The fitting of the HR C1s photoelectron peaks (figure SI3) of Bi_2O_3 (WE/Bi_2O_3) and CS@Bi_2O_3 (WE/CS@Bi_2O_3) modified electrodes shows a quite similar surface of both electrodes in terms of carbonaceous components to respect the WE electrodes electrochemically pretreated in KOH, with a decrease of the C—O contribution. The ratio between the carbon content and the carbonaceous oxygen content, obtained excluding the oxygen bonded to bismuth, is 4.3 and 5.2 respectively, showing a worthy increment to respect anodized WE/KOH. Otherwise, the oxygen spectrum near the epoxy/alkoxy peak shows a new component at 530.7 ± 0.1 eV that can be associated to carbonyl or quinones [32] with a contribution from the Bi_2O_3. As matter of the fact, in both samples a well resolved pair of peaks for Bi4f signal, with $Bi4f_{7/2}$ at 159.2 ± 0.1 eV and $Bi4f_{5/2}$ at 164.2 ± 0.1 eV, respectively (see figure SI4, panel A and B), clearly attributed to Bi_2O_3 (NIST database) is observed. Near these intense characteristic pair of peaks samples shows a pair of peaks at 157.2 ± 0.1 eV ($Bi4f_{7/2}$) and 162.1 ± 0.1 eV ($Bi4f_{5/2}$) attributed to a Bi(0) (NIST database). Typically, the Bi(0) component represents almost the 3.2 % of the Bi(III) content in absence of chitosan samples. A similar behaviour, suggest that the shell of the nanostructures is dominated from the Bi_2O_3, while the Bi(0) signal could be representative of a metallic core–shell. Probably the reduced bismuth form generated at −1.2 V is not stable and re-oxidized in air before XPS analysis. Regarding the chitosan, it is important to point out that in HR N1s region a very weak signal is observed only on CS@Bi_2O_3 sample. This data, also considering the attenuation of the Bi4f signals to respect Bi_2O_3 can confirm their presence. No information can be obtained from O1s and C1s signals, both dominated from the graphite base of the electrodes.

3.5. Bismuth oxide modified WE and Bi_2O_3/CS NSs modified WE: Electrochemical performance

To investigate the sensitivity in the simultaneous detection of Cd(II) and Pb(II), the parameters affecting the electroanalytical performance have been optimized. The SPE modified with Bi_2O_3 was tested in KCl 0.1 M pH 2.2 and in acetate buffer pH 4.5. It showed a mean better performance in the acetate buffer pH 4.5, with regard to linearity and limit of detection (LOD). A LOD of 1.7 μg L^{-1} and 0.5 μg L^{-1} for Cd(II) and Pb (II) respectively was observed, whereas a LOD of 2.8 μg L^{-1} and 0.1 μg L^{-1} for Cd(II) and Pb(II) respectively was observed in KCl 0.1 M, pH 2.2. The limit was calculated using the IUPAC definition [33] to derive the smallest measure, xL that can be detected, as shown below:

$$x_L = x_{bi} + ks_{bi}$$

where x_{bi} and s_{bi} are the mean and the standard deviation of the blank measures, respectively. The numerical factor k has been considered k = 3. Next, using the calibration slope, the corresponding concentration was found. As shown in Fig. 7 the sensor showed linearity in the range of (2–20) μg L^{-1} for Cd(II) ($R^2 = 0.997$) and in the range of (2–20) μg L^{-1} for Pb(II) ($R^2 = 0.999$) in acetate buffer/KCl pH 4.5. It is to be noted that after the electrochemical reduction step, reoxidation of a portion of bismuth in air occurs, as observed from the XPS data. However, during the stripping analysis, the bismuth oxide is reduced during the deposition step. In fact, in acetate buffer pH 4.5 the applied deposition potential of −1.2 V is sufficiently negative to electrochemically reduce the thin bismuth oxide layer formed over the WE [34].

Regarding the measurements in KCl 0.1 M, pH 2.2, the sensor showed linearity in the range of (3–15) μg L^{-1} for Cd(II) ($R^2 = 0.993$) and in the range of (5–20) μg L^{-1} for Pb(II) ($R^2 = 0.997$), as shown in Fig. 8.

Concerning the electrode modified with CS@Bi_2O_3 NSs, it was tested in acetate buffer pH 4.5 and it showed a LOD of 1.5 μg L^{-1} and 0.2 μg L^{-1} for Cd(II) and Pb(II), respectively. As reported in Fig. 9, the sensor showed linearity in the range of (2–20) μg L^{-1} for Cd(II) ($R^2 = 0.990$) and in the range of (2–20) μg L^{-1} for Pb(II) ($R^2 = 0.998$).

3.6. Reproducibility

Reproducibility was evaluated in the simultaneous detection of 5 μg/L of Cd(II) and Pb(II) in acetate buffer solution pH 4.5, based on 5 electrodes. An improvement in the reproducibility of Cd(II) detection was observed with the CS@Bi_2O_3 NSs-modified electrode compared to the bismuth oxide-modified electrode. Concerning the CS@Bi_2O_3 NSs modified electrode, the relative standard deviation was 13 % and 14 % for Cd(II) and Pb(II), respectively, whereas for the bismuth oxide-modified electrode it was 23 % for Cd(II) and 14 % for Pb(II).

3.7. Comparison with the unmodified graphite electrode and literature data

Modified electrodes show enhanced sensitivity than pristine graphite electrode in simultaneous detection of Cd(II) and Pb(II), especially for Cd(II) whose traces are more difficult to detect. Below, in Figs. 10-11, the comparison between the two modified electrodes and the unmodified graphite electrode is shown. The comparison concerns the simultaneous detection of 5 μg L^{-1} of Cd(II) and Pb(II) in acetate buffer pH 4.5. At these concentrations, the non-modified graphite electrode failed to detect Cd(II), whereas for Pb(II) it showed two peaks compared to the modified electrodes. The Pb(II) peak 2 would be determined by the underpotential deposition effect [35].

To further valuate the obtained results, different modification strategies (Table 1) were selected from literature with respect of bismuth graphite SPE and compared, while considering similar electrolyte conditions and square wave anodic stripping voltammetry as the electroanalytical technique applied to simultaneously detect Cd(II) and Pb(II) ions in water. Concerning those results with at least partially overlapping linearity ranges (where stated), the LOD values obtained for Cd (II) in our work are quite comparable [13-b; 36-a] better [13-a; 36-b; 38] or worst [41] without taking into account the different measurement conditions; the LOD values obtained for Pb(II) in our work resulted better than those reported by all the works cited in Table 1 except for the sparking approach [41]. The distribution of bismuth particles onto the carbonaceous surface or within the graphitic paste of the working electrode seems to be one of the critical issues determining the observed differences.

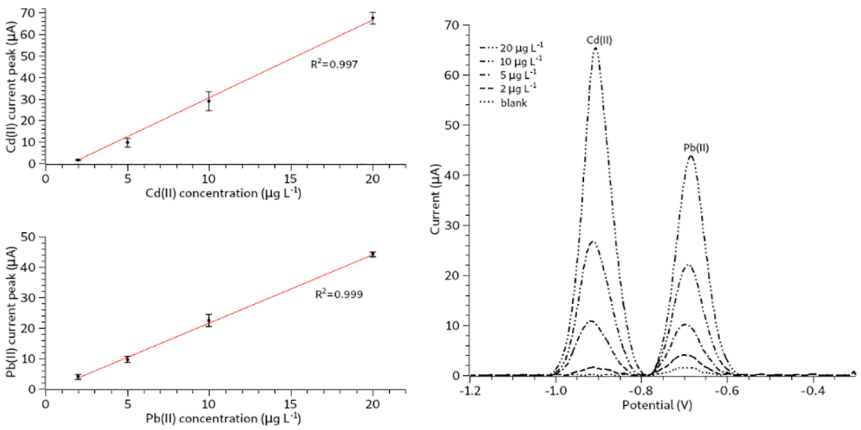

Fig. 7. Bi_2O_3 modified SPE. Detection of 2, 5, 10, 20 μg/L of Cd(II) and Pb(II) in acetate buffer/KCl solution, pH 4.5 (linearity on the left, SWV on the right).

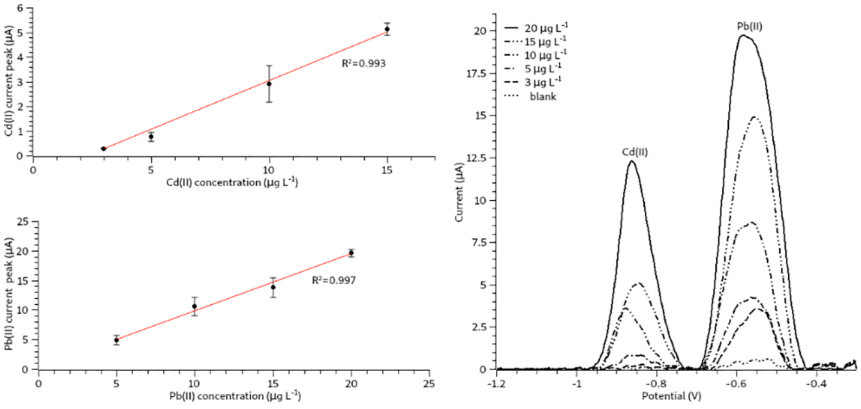

Fig. 8. Bi_2O_3 modified SPE. Detection of 3, 5, 10, 15, 20 μg/L of Cd(II) and Pb(II) in KCl 0.1 M, pH 2.2 (linearity on the left, SWV on the right).

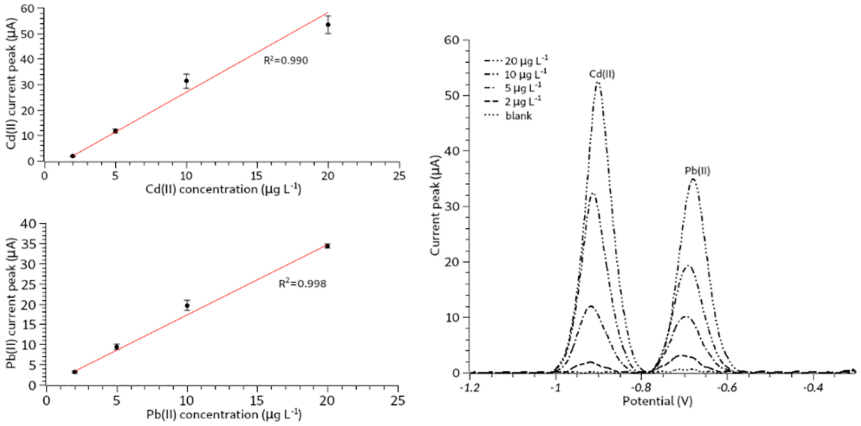

Fig. 9. Bi_2O_3CS NSs modified SPE. Detection of 2, 5, 10, 20 μg/L of Cd(II) and Pb(II) in acetate buffer/KCl solution, pH 4.5 (linearity on the left, SWV on the right).

3.8. Analysis of real samples

The bismuth-modified electrode was tested in the detection of Cd(II) and Pb(II) ions in ground water sample obtained in the framework of HydroRiskLab project (Bando INNOLABS – Sostegno alla creazione di soluzioni innovative finalizzate a specifici problemi di rilevanza sociale – Regione Puglia) from the project partner Consorzio Bonifica Montana del Gargano – Foggia. The water sample stored in the freezer at −20 °C was thawed. No filtration or chemical-physical digestion of the sample was carried out. Before the measurement, the pH of the underground water was adjusted to pH 4.5 using acetic acid and sodium acetate. The final sodium acetate concentration was 0.1 M.

As confirmed by gold standard method carried out in an external certified laboratory, Cd(II) and Pb(II) ions were not detectable in the ground water sample analyzed (Fig. 12). In addition, a blank measurement in acetate buffer/KCl pH 4.5 (prepared in ultrapure water) was also reported. Two measurements were then carried out by adding 5 μg L^{-1} of Cd(II) and Pb(II) (in the first measurement) and 10 μg L^{-1} of Cd (II) and Pb(II) (in the second measurement) to the ground water sample. The Bi-modified sensor responded as expected to the additions of Cd(II) and Pb(II) ions in a matrix with the presence of other interfering compounds.

Table 1
Comparison with representative literature data concerning the modification of SPE with bismuth or bismuth precursor for the detection of Pb(II) and Cd(II) by ASV.

Modification	Analyte	Electrolyte	Accumulation time	Linear range	LOD	Ref.
bulk with bismuth nanoparticle porous carbon nanocomposite	Pb(II) Cd(II)	0.1 M acetate buffer (pH 4.5)	90 s	(5–100) μg L^{-1} (5–100) μg L^{-1}	3.9 μg L^{-1} 2.1 μg L^{-1}	[13]-a
bulk with bismuth nanoparticle porous carbon nanocomposite	Pb(II) Cd(II)	0.1 M acetate buffer (pH 4.5)	300 s	(1–50) μg L^{-1} (1–50) μg L^{-1}	2.3 μg L^{-1} 1.5 μg L^{-1}	[13]-b
bulk with Bi_2O_3	Pb(II) Cd(II) Zn(II)	0.1 M HCl (ca. pH 1.2)	120 s	(5–150) μg L^{-1} (5–150) μg L^{-1} –	5 μg L^{-1} 2.5 μg L^{-1} –	[36]-a
bulk with Bi_2O_3	Pb(II) Cd(II) Zn(II)	0.1 M sodium acetate solution (ca. pH 4.5)	120 s	(10–150) μg L^{-1} (10–150) μg L^{-1} (10–150) μg L^{-1}	10 μg L^{-1} 5 μg L^{-1} 30 μg L^{-1}	[36]-b
ex-situ with $Bi(NO_3)_3$	Cd(II)	0.2 M acetate buffer (pH 4.5)	120 s	–	1.3 μg L^{-1}	[37]
bulk with bismuth powder	Cd(II)	acetate buffer (pH 4.0)	150 s	(5–50) μg L – 1	4.8 μg L – 1	[38]
screen-printing of Bi_2O_3	Pb(II) Cd(II)	0.1 M acetate buffer (pH 4.5)	300 s	(20–100) μg L^{-1} (20–100) μg L^{-1}	2.3 μg L^{-1} 1.5 μg L^{-1}	[39]
drop-casting of bismuth nanoparticles	Pb(II) Cd(II) Zn(II)	0.1 M acetate buffer (pH 4.5)	120 s	– – –	0.9 μg L^{-1} 1.3 μg L^{-1} 2.6 μg L^{-1}	[40]
Bi_2O_3 by sparking process	Pb(II) Cd(II)	0.1 M acetate buffer (pH 4.5)	120 s	(0–12) μg L^{-1} (0–12) μg L^{-1}	0.2 μg L^{-1} 0.2 μg L^{-1}	[41]
bulk with bismuth citrate	Pb(II) Cd(II)	0.1 M acetate buffer (pH 4.5)	120 s	– –	0.9 μg L^{-1} 1.1 μg L^{-1}	[42]
bulk with Bi_2O_3	Pb(II) Cd(II)	0.1 M acetate buffer (pH 4.5)	120 s	– –	1.0 μg L^{-1} 2.0 μg L^{-1}	[42]
drop-casting of Bi_2O_3 nanopowder	Pb(II) Cd(II)	acetate buffer/KCl solution (pH 4.5)	300 s	(2–20) μg L^{-1} (2–20) μg L^{-1}	0.5 μg L^{-1} 1.7 μg L^{-1}	this work-a
drop-casting of Bi_2O_3 nanopowder	Pb(II) Cd(II)	0.1 M KCl (pH 2.2)	300 s	(5–20) μg L^{-1} (3–15) μg L^{-1}	0.1 μg L^{-1} 2.8 μg L^{-1}	this work-b
drop-casting of chitosan coated Bi_2O_3 nanostructures	Pb(II) Cd(II)	acetate buffer/KCl solution (pH 4.5)	300 s	(2–20) μg L^{-1} (2–20) μg L^{-1}	0.2 μg L^{-1} 1.5 μg L^{-1}	this work

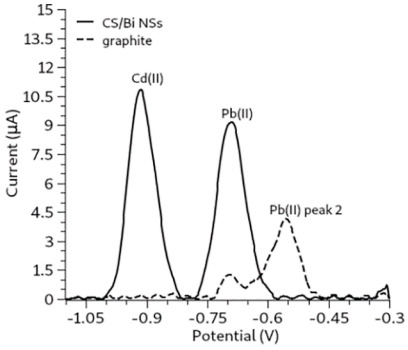

Fig. 10. Anodic stripping SWV. Comparison between the CS/Bi NSs modified electrode and the pristine graphite electrode detecting 5 μg L^{-1} of Cd(II) and Pb (II) in acetate buffer/KCl solution, pH 4.5.

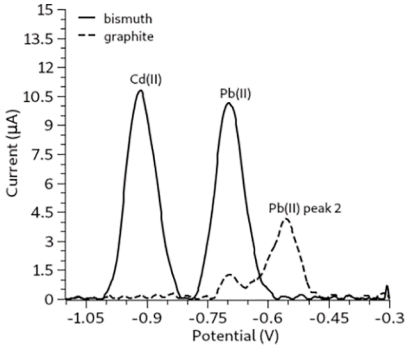

Fig. 11. Anodic stripping SWV. Comparison between the bismuth modified electrode and the pristine graphite electrode detecting 5 μg L^{-1} of Cd(II) and Pb (II) in acetate buffer/ KCl solution, pH 4.5.

4. Conclusions

In this work, a simple and environmentally friendly way of modifying a graphite SPE for metal ion detection was depicted. The method was optimized by drop deposition of bismuth oxide aqueous suspension onto the graphite WE, followed by electrochemical reduction of the bismuth oxide to obtain a bismuth layer on the WE surface; parameters for both electrode modification and anodic stripping SWV setting were thoroughly optimized for obtaining appropriate responses for Pb(II) and Cd(II). It allowed to improve the performance of the GSPE in the simultaneous detection of Cd(II) and Pb(II) ions. Besides, the use of CS@Bi_2O_3 hybrid NSs improved the sensor efficiency in terms of reproducibility for Cd(II) ions detection. μ-XRF analysis confirmed the stability of the coating even after the bismuth oxide reduction step carried out by GSPE immersion in KOH 0.1 M, under a potential of −1.2 V (vs Ag/AgCl RE) applied for 5 min. The GSPE modified with bismuth oxide suspension showed a LOD of 1.7 μg L^{-1} and 0.5 μg L^{-1} for Cd(II) and Pb(II) respectively, whereas the SPE modified with CS@Bi_2O_3 NSs suspension showed a LOD of 1.5 μg L^{-1} for Cd(II) and 0.2 μg L^{-1} for Pb (II) with linearity in the range of (2–20) μg L^{-1}.

Collected data arise from, and are influenced by, pristine GSPE composition (here deeply investigated by μ-XRF and XPS), and Bi modified electrodes show enhanced sensitivity than bare electrode in simultaneous detection of Cd(II) and Pb(II). Remarkably, considering

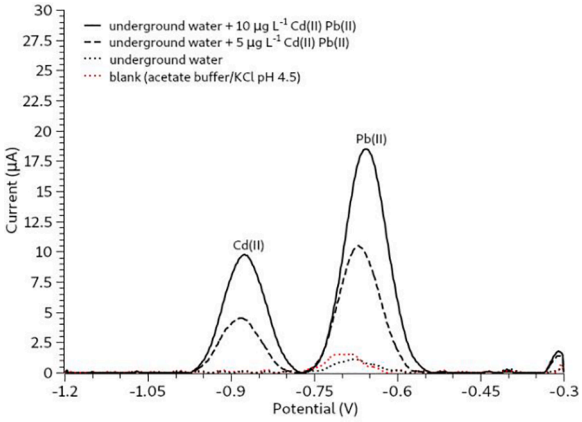

Fig. 12. Anodic stripping SWV in underground water using bismuth-modified GSPE.

literature data concerning bismuth or its oxide as (much cheaper) precursor, to modify the graphitic WE with different approaches and functional distributions, comparable or lower LOD (in line with the last EU Directive and WHO Water Safety Plan) were obtained in this study. The developed Bi–GSPE has been successfully applied in a spike test of known concentrations of metal ions in ground costal water to be conveyed into the irrigation network; measurements on real sample displayed remarkable peak resolution in a complex matrix, showing the applicability of such a nontoxic Bi-modified sensor for quality assurance in agronomic/environmental applications.

CRediT authorship contribution statement

Angelantonio De Benedetto: Writing – review & editing, Writing – original draft, Investigation, Formal analysis. **Antonio Della Torre:** Writing – review & editing, Writing – original draft, Formal analysis. **Maria Rachele Guascito:** Writing – review & editing, Writing – original draft, Resources, Formal analysis. **Riccardo Di Corato:** Formal analysis, Writing – review & editing. **Laura Chirivì:** Writing – review & editing. **Rosaria Rinaldi:** Writing – review & editing, Resources, Funding acquisition. **Alessandra Aloisi:** Writing – review & editing, Writing – original draft, Supervision, Investigation, Funding acquisition, Formal analysis, Conceptualization.

Declaration of competing interest

The authors declare that they have no known competing financial interests or personal relationships that could have appeared to influence the work reported in this paper.

Acknowledgements

This research was funded by DEDALO Project (F/200073/01- 03/X45) - MISE and Hydrorisklab Project (NRNABW5) – POR Puglia FESR-FSE 2014-2020.

A.D.B., A.A. and R.R. are grateful to MUR for a PhD grant financed by PON project “Dottorati innovativi con caratterizzazione industriale” (Code: project n.3 DOT1312457).

A.A. is grateful to Consorzio Bonifica Montana del Gargano – Foggia, Italy, for ground water samples providing.

Appendix A. Supplementary data

Supplementary data to this article can be found online at https://doi.org/10.1016/j.jelechem.2024.118341.

References

[1] Protecting Groundwater for Health Managing the Quality of Drinking-water Sources. Edited by O. Schmoll, G. Howard, J. Chilton and I. Chorus. World Health Organization (WHO) 2006. ISBN13: 9781843390794 (IWA Publishing).
[2] C. Kokkinos, A. Economou, Stripping Analysis at Bismuth-Based Electrodes, Curr. Anal. Chem. 4 (3) (2008) 183–190, https://doi.org/10.2174/157341108784911352.
[3] J. Wang, Stripping Analysis at Bismuth Electrodes: A Review, Electroanalysis 17 (2005) 1341–1346, https://doi.org/10.1002/elan.200403270.
[4] C. Ariño, N. Serrano, J.M. Díaz-Cruz, M. Esteban, Voltammetric determination of metal ions beyond mercury electrodes. A review, Anal. Chim. Acta 990 (2017) 11–53, https://doi.org/10.1016/j.aca.2017.07.069.
[5] C. Ariño, C.E. Banks, A. Bobrowski, R.D. Crapnell, A. Economou, A. Królicka, C. Pérez-Ràfols, D. Soulis, J. Wang, Electrochemical stripping analysis, Nat Rev Methods Primers 2 (2022) 62, https://doi.org/10.1038/s43586-022-00143-5.
[6] G.S. Ustabasi, M. Ozcan, I. Yilmaz, Review—Voltammetric Determination of Heavy Metals with Carbon-Based Electrodes, J. Electrochem. Soc. 168 (2021) 097508, https://doi.org/10.1149/1945-7111/ac253e.
[7] S.B. Hocevar, B. Ogorevc, J. Wang, in YISAC'00: 7th Young Investigators' Seminar on Analytical Chemistry, UNI Graz, Graz, Austria, Book of Abstracts, 2000, p. 19.
[8] N. Serrano, A. Alberich, J.M. Díaz-Cruz, C. Ariño, M. Esteban, Coating methods, modifiers and applications of bismuth screen-printed electrodes, TrAC, Trends Anal. Chem. 46 (2013) 15–29, https://doi.org/10.1016/j.trac.2013.01.012.
[9] A. Economou, Bismuth-film electrodes: recent developments and potentialities for electroanalysis, TrAC, Trends Anal. Chem. 24 (2005) 334–340, https://doi.org/10.1016/j.trac.2004.11.006.
[10] V. Sosa, N. Serrano, C. Ariño, J.M. Díaz-Cruz, M. Esteban, Sputtered bismuth screen-printed electrode: A promising alternative to other bismuth modifications in the voltammetric determination of Cd(II) and Pb(II) ions in groundwater, Talanta 119 (2014) 348–352, https://doi.org/10.1016/j.talanta.2013.11.032.
[11] M.A. Tapia, C. Pérez-Ràfols, R. Gusmão, N. Serrano, Z. Sofer, J.M. Díaz-Cruz, Enhanced voltammetric determination of metal ions by using a bismuthene-modified screen-printed electrode, Electrochim. Acta 362 (2020) 137144, https://doi.org/10.1016/j.electacta.2020.137144.
[12] R.O. Kadara, I.E. Tothill, Development of disposable bulk-modified screen-printed electrode based on bismuth oxide for stripping chronopotentiometric analysis of lead (II) and cadmium (II) in soil and water samples, Anal. Chim. Acta 623 (2008) 76–81, https://doi.org/10.1016/j.aca.2008.06.010.
[13] P. Niu, C. Fernández-Sánchez, M. Gich, C. Navarro-Hernández, P. Fanjul-Bolado, A. Roig, Screen-printed electrodes made of a bismuth nanoparticle porous carbon nanocomposite applied to the determination of heavy metal ions, Microchim. Acta 183 (2016) 617–623, https://doi.org/10.1007/s00604-015-1684-4.
[14] A. Economou, Recent developments in on-line electrochemical stripping analysis—An overview of the last 12 years, Anal. Chim. Acta 683 (2010) 38–51, https://doi.org/10.1016/j.aca.2010.10.017.
[15] I. Švancara, C. Prior, S.B. Hočevar, J. Wang, A Decade with Bismuth-Based Electrodes in Electroanalysis, Electroanalysis 22 (2010) 1405–1420, https://doi.org/10.1002/elan.200970017.
[16] V. Jovanovski, S.B. Hočevar, B. Ogorevc, Bismuth electrodes in contemporary electroanalysis, Curr. Opin. Electrochem. 3 (2017) 114–122, https://doi.org/10.1016/j.coelec.2017.07.008.
[17] A. García-Miranda Ferrari, P. Carrington, S.J. Rowley-Neale, C.E. Banks, Recent advances in portable heavy metal electrochemical sensing platforms, Environ. Sci. Water Res. Technol. 6 (2020) 2676–2690, https://doi.org/10.1039/D0EW00407C.
[18] Directive (EU) 2020/2184 of the European Parliament and of the Council of 16 December 2020 on the quality of water intended for human consumption (recast) (Text with EEA relevance) https://eur-lex.europa.eu/eli/dir/2020/2184/oj (accessed July 2023).
[19] Guidelines for drinking-water quality, 4th ed., incorporating the 1st addendum, https://www.who.int/publications/m/item/guidelines-for- drinking-water-quality-4th-ed.-incorporating-the-1st- addendum-(chapters) (accessed July 2023).
[20] M.E. Rice, Z. Galus, R.N. Adams, Graphite paste electrodes: Effects of paste composition and surface states on electron-transfer rates, J. Electroanal. Chem. Interfacial Electrochem. 143 (1983) 89–102, https://doi.org/10.1016/S0022-0728(83)80256-3.
[21] M. Pourbaix, Atlas of electrochemical equilibria in aqueous solutions, National Association of Corrosion Engineers (1974).
[22] T. Ernst, T. Berman, J. Buscaglia, T. Eckert-Lumsdon, C. Hanlon, K. Olsson, C. Palenik, S. Ryland, T. Trejos, M. Valadez, J.R. Almirall, Signal-to-noise ratios in forensic glass analysis by micro X-ray fluorescence spectrometry, X-Ray Spectrom. 43 (2014) 13–21, https://doi.org/10.1002/xrs.2437.
[23] D. Chirizzi, D. Mastrogiacomo, P. Semeraro, F. Milano, A.R. De Bartolomeo, M. Trotta, L. Valli, L. Giotta, M.R. Guascito, Nickel ion extracellular uptake by the phototrophic bacterium Rhodobacter sphaeroides: new insights from Langmuir modelling and X-ray photoelectron spectroscopic analysis, Appl. Surf. Sci. 593 (2022) 153385, https://doi.org/10.1016/j.apsusc.2022.153385.
[24] P. Pagliara, D. Chirizzi, M.R. Guascito, Chemical characterization of red cells from the black sea urchin *Arbacia lixula* by X-ray photoelectron spectroscopy, RSC Adv. 11 (2021) 27074–27083, https://doi.org/10.1039/D1RA03156B.
[25] NIST, X-Ray Photoelectron Spectroscopy Database, https://srdata.nist.gov/xps/main_search_menu.aspx, 2012 (accessed 2 January 2022).
[26] D. Briggs, M.P. Seah, Practical Surface Analysis: Auger and X-Ray Photoelectron Spectroscopy, J. Wiley Press, Chichester, 1990, pp. 151–152.
[27] V. Vivier, C. Cachet-Vivier, S. Mezaille, B.L. Wu, C.S. Cha, J.-Y. Nedelec, M. Fedoroff, D. Michel, L.T. Yu, Electrochemical Study of Bi_2O_3 and $Bi_2O_2CO_3$ by

Means of a Cavity Microelectrode I. Observed Phenomena and Direct Analysis of Results, J. Electrochem. Soc. 147 (2000), https://doi.org/10.1149/1.1394049.
[28] V. Vivier, A. Régis, G. Sagon, J.-Y. Nedelec, L.T. Yu, C. Cachet-Vivier, Cyclic voltammetry study of bismuth oxide Bi_2O_3 powder by means of a cavity microelectrode coupled with Raman microspectrometry, Electrochim. Acta 46 (2001) 907–914, https://doi.org/10.1016/S0013-4686(00)00677-0.
[29] H. Zhang, C. Lin, L. Sepunaru, C. Batchelor-McAuley, R.G. Compton, Oxygen reduction in alkaline solution at glassy carbon surfaces and the role of adsorbed intermediates, J. Electroanal. Chem. 799 (2017) 53–60, https://doi.org/10.1016/j.jelechem.2017.05.037.
[30] F.E. Galdino, J.P. Smith, S.I. Kwamou, D.K. Kampouris, J. Iniesta, G.C. Smith, J. A. Bonacin, C.E. Banks, Graphite Screen-Printed Electrodes Applied for the Accurate and Reagentless Sensing of pH, Anal. Chem. 87 (2015) 11666–11672, https://doi.org/10.1021/acs.analchem.5b01236.
[31] D.J. Morgan, Comments on the XPS Analysis of Carbon Materials, C 7 (2021) 51, https://doi.org/10.3390/c7030051.
[32] M. Pedrosa, E.S. Da Silva, L.M. Pastrana-Martínez, G. Drazic, P. Falaras, J.L. Faria, J.L. Figueiredo, A.M.T. Silva, Hummers' and Brodie's graphene oxides as photocatalysts for phenol degradation, J. Colloid Interface Sci. 567 (2020) 243–255, https://doi.org/10.1016/j.jcis.2020.01.093.
[33] IUPAC. Compendium of Chemical Terminology, 2nd ed. (the "Gold Book"). Compiled by A. D. McNaught and A. Wilkinson. Blackwell Scientific Publications, Oxford, 1997. Online version (2019-) created by S. J. Chalk. ISBN 0-9678550-9-8. DOI: 10.1351/goldbook.
[34] R. Pauliukaite, R. Metelka, I. Švancara, A. Królicka, A. Bobrowski, K. Vytřas, E. Norkus, K. Kalcher, Carbon paste electrodes modified with Bi_2O_3 as sensors for the determination of Cd and Pb, Anal. Bioanal. Chem. 374 (2002) 1155–1158, https://doi.org/10.1007/s00216-002-1569-3.
[35] T. Navrátil, J. Barek, M. Kopanica, Anodic stripping voltammetry using graphite composite solid electrode, Collect. Czech. Chem. Commun. 74 (2009) 1807–1826, https://doi.org/10.1135/cccc2009107.
[36] R.O. Kadara, N. Jenkinson, C.E. Banks, Disposable Bismuth Oxide Screen Printed Electrodes for the High Throughput Screening of Heavy Metals, Electroanalysis 21 (2009) 2410–2414, https://doi.org/10.1002/elan.200900266.
[37] O. Zaouak, L. Authier, C. Cugnet, A. Castetbon, M. Potin-Gautier, Bismuth-Coated Screen-Printed Microband Electrodes for On-Field Labile Cadmium Determination, Electroanalysis 21 (2009) 689–695, https://doi.org/10.1002/elan.200804465.
[38] C. Zhang, C. Li, X. Han, Screen printed electrode containing bismuth for the detection of cadmium ion, J. Electroanal. Chem. 933 (2023) 117291, https://doi.org/10.1016/j.jelechem.2023.117291.
[39] G.-H. Hwang, W.-K. Han, J.-S. Park, S.-G. Kang, An electrochemical sensor based on the reduction of screen-printed bismuth oxide for the determination of trace lead and cadmium, Sens. Actuators B 135 (2008) 309–316, https://doi.org/10.1016/j.snb.2008.08.039.
[40] M.Á.G. Rico, M. Olivares-Marín, E.P. Gil, Modification of carbon screen-printed electrodes by adsorption of chemically synthesized Bi nanoparticles for the voltammetric stripping detection of Zn(II), Cd(II) and Pb(II), Talanta 80 (2009) 631–635, https://doi.org/10.1016/j.talanta.2009.07.039.
[41] D. Riman, D. Jirovsky, J. Hrbac, M.I. Prodromidis, Green and facile electrode modification by spark discharge: Bismuth oxide-screen printed electrodes for the screening of ultra-trace Cd(II) and Pb(II), Electrochem. Commun. 50 (2015) 20–23, https://doi.org/10.1016/j.elecom.2014.11.003.
[42] N. Lezi, A. Economou, P.A. Dimovasilis, P.N. Trikalitis, M.I. Prodromidis, Disposable screen-printed sensors modified with bismuth precursor compounds for the rapid voltammetric screening of trace Pb(II) and Cd(II), Anal. Chim. Acta 728 (2012) 1–8, https://doi.org/10.1016/j.aca.2012.03.036.